

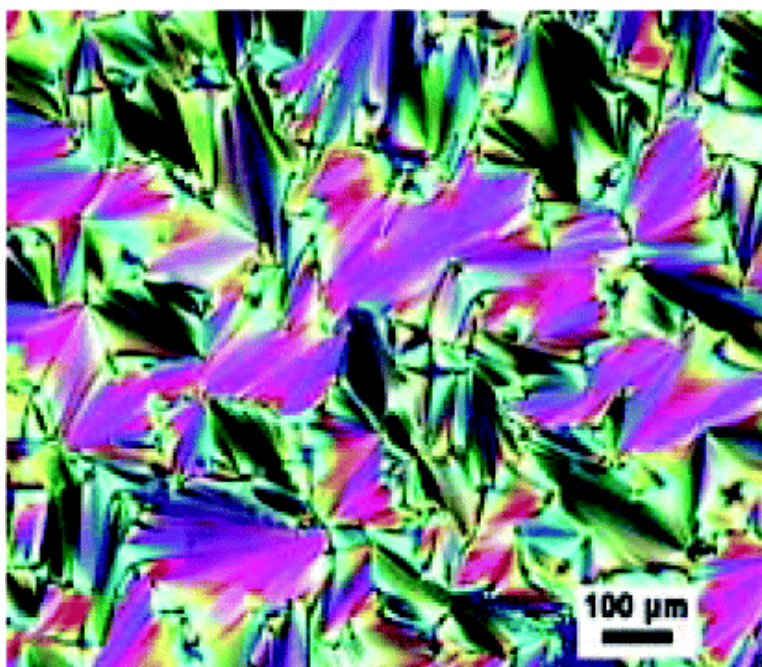
## Article

### Novel Ionic Liquid Crystals Based on *N*-Alkylcaprolactam as Cations

Jing Yang, Qinghua Zhang, Laiying Zhu, Shiguo Zhang, Jian Li, Xiaoping Zhang, and Youquan Deng

*Chem. Mater.*, **2007**, 19 (10), 2544-2550 • DOI: 10.1021/cm062675s • Publication Date (Web): 20 April 2007

Downloaded from <http://pubs.acs.org> on February 25, 2009



## More About This Article

Additional resources and features associated with this article are available within the HTML version:

- Supporting Information
- Links to the 1 articles that cite this article, as of the time of this article download
- Access to high resolution figures
- Links to articles and content related to this article
- Copyright permission to reproduce figures and/or text from this article

[View the Full Text HTML](#)



**ACS Publications**  
High quality. High impact.

## Novel Ionic Liquid Crystals Based on *N*-Alkylcaprolactam as Cations

Jing Yang,<sup>†,‡,§</sup> Qinghua Zhang,<sup>†,‡</sup> Laiying Zhu,<sup>†</sup> Shiguo Zhang,<sup>†</sup> Jian Li,<sup>†</sup>  
Xiaoping Zhang,<sup>‡</sup> and Youquan Deng<sup>\*,†</sup>

Centre for Green Chemistry and Catalysis, Lanzhou Institute of Chemical Physics, Chinese Academy of Sciences, Lanzhou 730000, China, School of Information Science and Engineering and The National Laboratory of Applied Organic Chemistry, Lanzhou University, Lanzhou 73000, China, and Graduate School of the Chinese Academy of Sciences, Beijing 100039, China

Received November 9, 2006. Revised Manuscript Received March 1, 2007

A novel series of ionic liquids (ILs) based on *N*-alkyl- $\epsilon$ -caprolactam as cations [C<sub>*n*</sub>-CP]<sup>+</sup> (C<sub>*n*</sub> = alkyl with different numbers of C atoms; *n* = 6, 8, 10, 12, 16, or 18) containing toluene-*p*-sulfonate [TS]<sup>−</sup> and methanesulfonate [MS]<sup>−</sup> as anions have been synthesized via a one-step atom-economic reaction. Characterizations of these ILs by differential scanning calorimetry, polarizing optical microscopy, variable-temperature powder X-ray diffraction, etc., were conducted. The results showed that the caprolactam-based ILs (*n* ≥ 8) were enantiotropic thermotropic liquid crystals, except for C<sub>18</sub>-CPMS (monotropic), and displayed smectic A phases. Some properties, such as higher transition enthalpies (e.g.,  $\Delta H = 83.1$  kJ/mol for C<sub>18</sub>-CPTS), higher specific heat capacities (e.g.,  $C_p = 2.85$  J/g·K for C<sub>16</sub>-CPTS) and higher heat storage densities (e.g., sensible heat storage density  $E_s = 262.81$  MJ/m<sup>3</sup> for C<sub>16</sub>-CPTS; latent heat storage density  $E_l = 146.0$  MJ/m<sup>3</sup> for C<sub>18</sub>-CPTS), were observed. Fluorescence measurements showed that the homologous C<sub>*n*</sub>-CPTS ILs exhibited strong fluorescence behavior. Finally, the test of acute toxicity toward rats showed that these new ILs were less toxic than the popular [BMIm]BF<sub>4</sub> IL.

### Introduction

Ionic liquids (ILs) are attracting considerable attention as versatile media and materials due to their peculiar physicochemical properties.<sup>1–3</sup> ILs could be “designer” soft media and materials with desired functions, and therefore, syntheses of ILs with unique physicochemical properties, particularly with extreme properties, such as lower melting point,<sup>4</sup> lower viscosity,<sup>5</sup> higher density,<sup>6</sup> and higher thermal stability,<sup>6</sup> etc., should be the hot topic of the current ILs research.

The most popular ILs, based on dialkylimidazolium and its derivatives, have been extensively studied and their corresponding properties—chemical,<sup>7</sup> electrical,<sup>8</sup> thermal,<sup>9</sup>

optical,<sup>10</sup> and even mechanical<sup>11</sup>—have been investigated and understood relatively well; therefore, to develop other ILs with peculiar physicochemical properties would be highly desirable.

Ionic liquid crystals (ILCs)<sup>12–15</sup> can be considered as materials that combine the properties of liquid crystals and ILs, which means that some of the properties of the ILCs differ significantly from those of conventional liquid crystals with neutral organic compounds.<sup>16,17</sup> They are anisotropic solvents and could be used as ordered reaction media that impart selectivity in reactions<sup>18</sup> or as templates for the

\* To whom correspondence should be addressed: fax +86-931-4968116; e-mail ydeng@lzb.ac.cn.

<sup>†</sup> Centre for Green Chemistry and Catalysis, Lanzhou Institute of Chemical Physics, Chinese Academy of Sciences.

<sup>‡</sup> School of Information Science and Engineering and The National Laboratory of Applied Organic Chemistry, Lanzhou University.

<sup>§</sup> Graduate School of the Chinese Academy of Sciences.

- (1) Welton, T. *Chem. Rev.* **1999**, *99*, 2071.
- (2) Wasserscheid, P.; Keim, W. *Angew. Chem., Int. Ed.* **2000**, *39*, 3772.
- (3) Sheldon, R. *Chem. Commun.* **2001**, 2399.
- (4) Wilkes, J. S. *Green Chem.* **2002**, *4*, 73.
- (5) Wilkes, J. S.; Zaworotko, M. J. *J. Chem. Soc., Chem. Commun.* **1992**, 965.
- (6) (a) Rogers, R. D.; Seddon, K. R., Eds. *Ionic Liquids IIIA*; ACS Symposium Series 901; American Chemical Society: Washington, DC, 2005. (b) Rogers, R. D.; Seddon, K. R. *Ionic Liquids: Industrial Applications to Green Chemistry*; Oxford University Press: New York, 2002. (c) Wasserscheid, P., Welton, T., Eds. *Ionic Liquids in Synthesis*, Wiley-VCH: Weinheim, Germany, 2003.
- (7) (a) Blanchard, L. A.; Hancu, D.; Beckman, E. J.; Brennecke, J. F. *Nature* **1999**, *399*, 28. (b) Huddleston, J. G.; Willauer, H. D.; Swatoski, R. P.; Visser, A. E.; Rogers, R. D. *Chem. Commun.* **1998**, 1765. (c) Visser, A. E.; Swatoski, R. P.; Rogers, R. D. *Green Chem.* **2000**, *2*, 1.

- (8) Dickinson, V. E.; Williams, M. S.; Hendrickson, S. M.; Masui, H.; Murray, R. W. *J. Am. Chem. Soc.* **1999**, *121*, 613.
- (9) (a) Bonhote, P.; Dias, A. P.; Papageorgiou, N.; Kalyanasundaram, K.; Gratzel, M. *Inorg. Chem.* **1996**, *35*, 1168. (b) Holbrey, J. D.; Seddon, K. R. *J. Chem. Soc., Dalton Trans.* **1999**, 2133. (c) Ngo, H. L.; Le Comte, H.; Hargens, L.; McEwen, A. B. *Thermochim. Acta* **2000**, *357–358*, 97. (d) Huddleston, J. G.; Visser, A. E.; Reichert, W. M.; Willauer, H. D.; Broker, G. A.; Rogers, R. D. *Green Chem.* **2001**, *3*, 156.
- (10) (a) Del Sesto, R. E.; Corley, C.; Robertson, A.; Wilkes, J. S. *J. Organomet. Chem.* **2005**, *690*, 2536. (b) Sesto, R.; Dudis, D.; Ghebremichael, F.; Heimer, N.; Low, T.; Wilkes, J. S.; Yeates, A. Linear and Nonlinear Optics of Organic Materials III. *Proc. SPIE* **2003**, 5212.
- (11) Ye, C. F.; Liu, W. M.; Chen, Y. X.; Yu, L. G. *Chem. Commun.* **2001**, 2244.
- (12) Demus, D.; Goodby, J.; Gray, C. W.; Spiess, H. W.; Vill, V. *Handb. Liq. Cryst., Amphiphilic Liq. Cryst.* **1998**, *3*, 303.
- (13) Blandamer, M. J.; Brigg, B.; Cullis, P. M. *Chem. Soc. Rev.* **1995**, 251.
- (14) Neve, F. *Adv. Mater.* **1996**, *8*, 277.
- (15) Jeffrey, G. A. *Acc. Chem. Res.* **1986**, *19*, 168.
- (16) (a) Gordon, C. M.; Holbrey, J. D.; Kennedy, A.; Seddon, K. R. *J. Mater. Chem.*, **1998**, *8*, 2627. (b) Holbrey, J. D.; Seddon, K. R. *J. Chem. Soc., Dalton Trans.*, **1999**, 2133.
- (17) Binnemans, K. *Chem. Rev.* **2005**, *105*, 4148.

synthesis of mesoporous materials,<sup>19</sup> nanomaterials,<sup>20</sup> or zeolitic materials.<sup>21</sup> ILCs are also very promising candidates to design anisotropic ion-conductive materials because they have an anisotropic structural organization and ionic character.<sup>17</sup> To this day, the number of ILCs is still rather limited, and the field has potential for a strong further expansion.

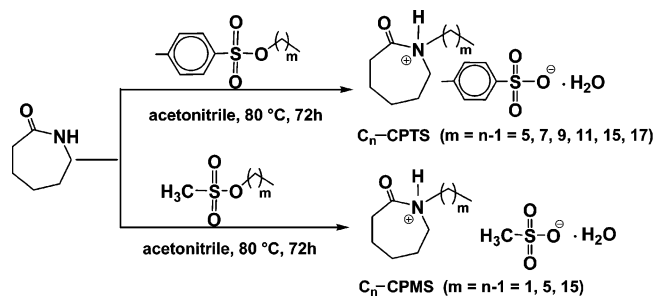
Caprolactam, which is relatively cheaper, has intrinsically lower toxicity, and is available on a large scale from industry, is a kind of amine derivative that could be quaternized to form new ionic compound cations with specific properties due to the carbonyl group on the caprolactam.<sup>22</sup> Recently, a series of caprolactam-cation-based Brønsted acid ILs have been synthesized and characterizations of the corresponding physicochemical properties were investigated preliminarily in our research group,<sup>23</sup> and these ILs could be used as effective catalysts and reaction media for Beckmann rearrangement of cyclohexanone oxime to afford caprolactam without using oleum.<sup>24</sup> In this work, we report our further research on caprolactam-cation-based ILs, that is, syntheses of ILs containing *N*-alkylcaprolactam  $[C_n\text{-CP}]^+$  ( $C_n$  = alkyl with different numbers of C atoms,  $n = 6, 8, 10, 12, 16,$  or  $18$ ) as cations and toluene-*p*-sulfonate  $[\text{TS}]^-$  or methanesulfonate  $[\text{MS}]^-$  as anions via a one-step atom-economic reaction. The study shows, depending on the number of C atoms of the alkyl chain on the caprolactam-based cation, that the shortest-chain ILs,  $C_6\text{-CPTS}$  and  $C_6\text{-CPMS}$ , melt into an isotropic liquid directly and no mesophase is observed. For  $n \geq 8$ , the ILs are thermotropic ionic liquid crystals with the usual smectic A phase, and their thermal properties are particularly focused and presented in addition to the preliminary measurements of fluorescence and toxicity.

## Experimental Section

**Materials.** All chemicals used in this work were of analytical grade and were used as received. *p*-Toluenesulfonyl chloride (or methanesulfonyl) and all alcohols were purchased from Shanghai Reagent Corp. Ltd. and Taijin Reagent Corporation Ltd., respectively.  $\epsilon$ -Caprolactam was purchased from Beijing Chemical Reagent Co.

**Methods.** The  $^1\text{H}$  NMR spectra were recorded on a Bruker AMX FT 400-MHz NMR spectrometer. Chemical shifts were reported in parts per million (ppm,  $\delta$ ). Elemental analyses were performed with a Elementar Analysensysteme GmbH VarioEL using the software version V3.00. Electrospray ionization (ESI<sup>+</sup>) mass spectra and infrared spectra were recorded on a Bruker Daltonics APEX

### Scheme 1. Preparation of the ILs Based on *N*-Alkylcaprolactam as Cations



II 47e Fourier transform mass spectrometer (FTMS) and a Thermo Nicolet 5700 Fourier transform infrared (FT-IR) spectrophotometer, respectively.

The densities ( $\rho$ ) were measured at 130 °C in a 2 mL volumetric flask calibrated with water by the mass method.

The thermal decomposition temperatures ( $T_d$ ) with 5% weight loss were assessed by employing a Beijing WCT-2C thermogravimetry (TG)/differential thermal analysis (DTA) instrument, and all samples for TG/DTA measurements were made with open  $\text{Al}_2\text{O}_3$  pans at a heating rate of 10 °C/min under a nitrogen atmosphere. Measurements of thermal analysis and phase-transition temperatures were done with a Mettler-Toledo DSC822<sup>e</sup> differential scanning calorimeter (DSC) at a scanning rate of 10 °C/min by applying several cooling and heating cycles from  $-50$  to  $150$  °C in a flowing nitrogen atmosphere; the samples were tightly sealed in aluminum pans. Melting points ( $T_{\text{mp}}$ ), freezing points ( $T_{\text{fp}}$ ) and clearing points ( $T_{\text{cp}}$ ) were the onset of peaks of DSC. A sapphire disk ( $\text{Al}_2\text{O}_3$ ) was used as the standard substance to determine the heat capacities ( $C_p$ ), and the data were evaluated by use of Mettler-Toledo STAR<sup>e</sup> software version 8.10. Optical micrographs were observed with a Nanjing XS-402P polarizing optical microscope (POM) equipped with a XMT-3000 heating stage and a temperature control unit, and a test wafer of gypsum as compensation background.

Powder X-ray diffraction (PXRD) experiments at different temperatures were conducted on a PANalytical X-ray diffraction system, the X'Pert PRO MPD with monochromatized  $\text{Cu K}\alpha$  ( $\lambda = 1.54$  Å) radiation from the high-voltage generator (operating at 40 kV, 40 mA), equipped with a X'Celerator detector and a TCU 2000 hot stage for heating. Data were recorded from  $3^\circ$  to  $30^\circ$  in steps of  $0.03^\circ$ .

The fluorescence spectra were recorded on a Hitachi model F-4500 FL spectrophotometer with a scan speed of 240 nm/min and PMT voltage 700 V at room temperature.

The preliminary comparison experiment of the toxicity have been conducted through an acute toxicity test toward the Kunming albino rats (17 – 22 g, adult). In each experiment, a dose of 0.4 mL aqueous solution or suspension containing 10 to 100 mg/mL of each IL was simultaneously fed to five male and five female rats through a feeding trough, and the relative toxicity of the ILs could be estimated through the comparison with the living time and death number of the rats.

**Synthesis of the ILs.** All the alkylmethanesulfonates, the alkyltoluene-*p*-sulfonates (Scheme 1) and the *N*-alkylcaprolactam-based ILs were prepared according to the literature procedures with a slight modification.<sup>25</sup> The synthetic processes of the new ILs are described below.

***N*-Octadecyl- $\epsilon$ -caprolactam Cation-Based Toluene-*p*-sulfonate- $[\text{C}_{18}\text{-CPTS}]$ .**  $\epsilon$ -Caprolactam (11.3 g, 0.1 mol) was dissolved in 30 mL of acetonitrile in a 250 mL three-necked round-bottomed

(18) Weiss, R. G. *Tetrahedron* **1988**, *44*, 3413.

(19) (a) Nishiyama, N.; Tanaka, S.; Egashira, Y.; Oku, Y.; Ueyama, K. *Chem. Mater.* **2003**, *15*, 1006. (b) Strawhecker, K. E.; Manias, E. *Chem. Mater.* **2003**, *15*, 844. (c) Brennan, T.; Hughes, A. V.; Roser, S. J.; Mann, S.; Edler, K. J. *Langmuir* **2002**, *18*, 9838. (d) Lin, H. P.; Mou, C. Y. *Acc. Chem. Res.* **2002**, *35*, 927.

(20) (a) Gilman, J. W.; Awad, W. H.; Davis, R. D.; Shields, J.; Harris, R. H., Jr.; Davis, C.; Morgan, A. B.; Sutto, T. E.; Callahan, J.; Trulove, P. C.; DeLong, H. C. *Chem. Mater.* **2002**, *14*, 3776. (b) Zhu, J.; Morgan, A. B.; Lamelas, F. J.; Wilkie, C. A. *Chem. Mater.* **2001**, *13*, 3774. (c) Li, L. S.; Walda, J.; Manna, L.; Alivisatos, A. P. *Nano Lett.* **2002**, *2*, 557.

(21) O'Regan, B.; Grätzel, M. *Nature* **1991**, *353*, 737.

(22) Demberlnyamba, D.; Bae, K. S.; Huen, L. *Chem. Commun.* **2002**, 1538.

(23) Du, Z. Y.; Li, Z. P.; Guo, S.; Zhang, J.; Zhu, L. Y.; Deng, Y. Q. *J. Phys. Chem. B* **2005**, *109*, 19542.

(24) Guo, S.; Du, Z. Y.; Zhang, S. G.; Li, D. M.; Li, Z. P.; Deng, Y. Q. *Green Chem.* **2006**, *8*, 1.

(25) Sekrea, V. C.; Marvel, C. S. *J. Am. Chem. Soc.*, **1933**, *55*, 345.

flask, and then a slight excess of octadecyl toluene-*p*-sulfonate [ $\text{CH}_3\text{-(C}_6\text{H}_4\text{)SO}_3\text{C}_{18}\text{H}_{37}$ ] (46.7 g, 0.11 mol) was added. The solution was stirred continuously under refluxing conditions at 70–80 °C for 72 h. After it was cooled to room temperature, the resulted yellowish mixture was filtered and recrystallized (3 $\times$ ) from ethyl acetate (3  $\times$  50 mL) and ethanol (3  $\times$  10 mL). The desired product was obtained as white crystals when the volatiles (ethyl acetate or ethanol) were removed under reduced pressure at 90–100 °C for 3 h (yield 44.6 g, 83%).  $^1\text{H NMR}$  (400 MHz, DMSO)  $\delta$ /ppm 0.86 (t,  $J = 6.6$  Hz, 3H), 1.24–1.56 (m, 38H), 2.29 (s, 3H), 2.29 (t,  $J = 7.4$  Hz, 2H), 2.76 ( $J = 6.8$  Hz, 2H), 3.99 (t,  $J = 6.6$  Hz, 2H), 7.11 (d,  $J = 8.0$  Hz, 2H), 7.47 (d,  $J = 8.4$  Hz, 2H), 7.6 (br s, 1H). MS (ESI $^+$ ) calcd  $m/z = 384.3836$  ( $\text{M}^+$ ,  $\text{C}_{24}\text{H}_{48}\text{NO}\cdot\text{H}_2\text{O}$ ); found  $m/z = 384.3842$  ( $\text{M}^+$ ,  $\text{C}_{24}\text{H}_{48}\text{NO}\cdot\text{H}_2\text{O}$ ). IR (KBr,  $\nu_{\text{cm}^{-1}}$ ) 1731. Anal. Calcd for  $\text{C}_{31}\text{H}_{55}\text{NSO}_4\cdot\text{H}_2\text{O}$ : C, 66.99; H, 10.34; N, 2.52. Found: C, 67.18; H, 9.84; N, 2.11.

**N-Hexadecyl- $\epsilon$ -caprolactam Cation-Based Methanesulfonate [ $\text{C}_{16}$ -CPMS].**  $\epsilon$ -Caprolactam (11.3 g, 0.1 mol) was dissolved in 30 mL of acetonitrile in a 250 mL three-necked round-bottomed flask, and then a slight excess of hexadecyl methanesulfonate [ $\text{CH}_3\text{-SO}_3\text{C}_{16}\text{H}_{33}$ ] (35.3 g, 0.11 mol) was added. The solution was stirred continuously under refluxing conditions at 70–80 °C for 72 h. After it was cooled to room temperature, the resulted yellowish mixture was filtered and recrystallized (3 $\times$ ) from ethyl acetate (3  $\times$  50 mL) and ethanol (3  $\times$  10 mL). The desired product was obtained as white crystals when the volatiles (ethyl acetate or ethanol) were removed under reduced pressure at 90–100 °C for 3 h (yield 30.7 g, 71%).  $^1\text{H NMR}$  (400 MHz, DMSO)  $\delta$ /ppm 0.86 (t,  $J = 6.6$  Hz, 3H), 1.24–1.56 (m, 34H), 2.29 (s, 3H), 2.29 (t,  $J = 5.4$  Hz, 2H), 2.76 ( $J = 5.6$  Hz, 2H), 3.99 (t,  $J = 6.6$  Hz, 2H), 7.6 (br s, 1H). MS (ESI $^+$ ) calcd  $m/z = 356.3523$  ( $\text{M}^+$ ,  $\text{C}_{22}\text{H}_{44}\text{NO}\cdot\text{H}_2\text{O}$ ); found  $m/z = 356.3527$  ( $\text{M}^+$ ,  $\text{C}_{22}\text{H}_{44}\text{NO}\cdot\text{H}_2\text{O}$ ). IR (KBr,  $\nu_{\text{cm}^{-1}}$ ) 1731. Anal. Calcd for  $\text{C}_{23}\text{H}_{47}\text{NSO}_4\cdot\text{H}_2\text{O}$ : C, 61.16; H, 10.93; N, 3.10. Found: C, 61.35; H, 10.51; N, 2.63.

## Results and Discussion

**Synthesis and Identification.** All nine ILs based on *N*-alkylcaprolactam as cations were synthesized in a one-step atom-economic reaction by mixing caprolactam and a slight excess of ester (molar ratio 1:1.1) in refluxing acetonitrile. The desired products were obtained with 70–90% yields as white crystals at room temperature, and as the alkyl chain length on the cation increased, the hydrophilicity/hydrophobicity of the ILs gradually decreased/increased. The structure identification with NMR, ESI-MS, FT-IR, elemental analyses, etc., is described in detail in Supporting Information (Figures S1–S7 and Table S1). Unexpectedly, the purified desired ILs contain one extra crystallized  $\text{H}_2\text{O}$  molecule as confirmed by ESI-MS and elemental analyses.

**Thermal Decomposition Temperatures.** A typical result of TG/DTA is shown in Figure 1. The decomposition thermograms of all caprolactam-based ILs were similar to this curve. The temperatures of thermal decomposition were in the range of 253–289 °C for a weight loss of 5%, slightly affected by the number of C atoms of the alkyl chain on the caprolactam and the variation of anions. The active carbonyl group on caprolactam may result in a decrease of the thermal stability, and due to the carbonyl group such ILs may be relatively easily degraded, making these ILs more attractive as environmentally benign media or soft material. In addition,

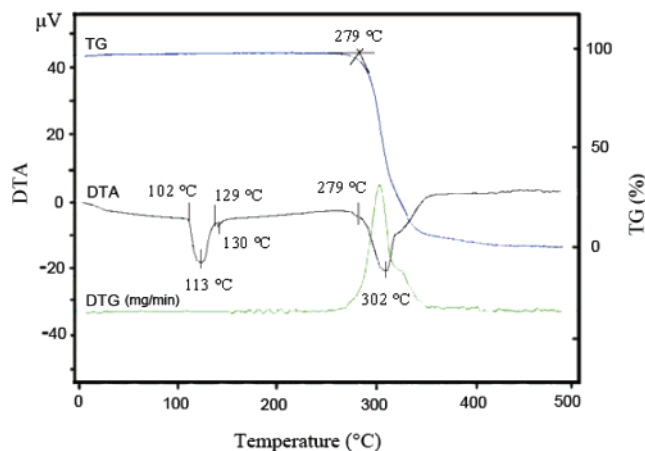


Figure 1. TG/DTA thermograms of  $\text{C}_{18}$ -CPTS.

the TG curves, depending on each IL, were almost flat until ca. 253–289 °C, suggesting that that one  $\text{H}_2\text{O}$  molecule contained in the IL was quite stable and that one  $\text{H}_2\text{O}$  molecule may combine with the IL until the thermal decomposition of whole IL.

**Thermotropic Property.** The phase behaviors of the two homologous series  $\text{C}_n$ -CPTS ( $n = 6, 8, 10, 12, 16, \text{ or } 18$ ) and  $\text{C}_n$ -CPMS ( $n = 6, 16, \text{ or } 18$ ) ILs were investigated with DSC, POM, and XRD.

**Differential Scanning Calorimetry.** DSC-derived data, transition temperatures, enthalpies ( $\Delta H$ ), entropies ( $\Delta S$ ), and supercooling ( $\Delta T_s$ ) for the studied ILs are given in Table 1. Their distinct melting points (83.5–127.4 °C) and freezing points (77.5–100.8 °C) were observed, which indicated that obvious sharp phase changes occurred during the transformation between solid and liquid over the ILs. Although the melting points are a little bit high, they should be a kind of ionic liquid on the basis of the structure and properties of the salts. The melting, freezing, and clearing points were affected by the number of carbon atoms of the alkyl chain on the caprolactam and the variation of anions; that is, the melting and freezing points increased with increasing chain length on cations or upon substituting  $[\text{TS}]^-$  with  $[\text{MS}]^-$  anion. At the same time, trivial supercoolings [ $\Delta T_s = 2.4$ –4.1 °C, except for  $\text{C}_8$ -CPTS (6.0 °C),  $\text{C}_{10}$ -CPTS (7.3 °C), and  $\text{C}_6$ -CPMS (26.6 °C)] were observed as the freezing points were slightly lower than the melting points, which were different from conventional ILs with extensive supercoolings.

It is interesting to note that the heating and cooling DSC cycle of  $\text{C}_{10}$ -CPTS shows three vivid exothermic and endothermic peaks, respectively (Figure 2). Upon cooling, a little peak with rather lower enthalpy value  $\Delta H = 2.6$  kJ/mol occurs at 108.2 °C in addition to two large peaks with higher enthalpy values, which correspond to the transition of crystal-to-crystal phase. The overlapping of melting and recrystallizing instantaneously resulted in formation of the complicated peaks, and the similar peak with lower enthalpy  $\Delta H = 2.3$  kJ/mol and entropy  $\Delta S = 5.9$  J/mol·K at 109.0 °C upon heating was observed (third section in Table 1).

The ILs with longer alkyl chains ( $n = 12, 16, \text{ or } 18$ ) exhibited similar DSC thermograms when melted from the

Table 1. Transition Temperatures, Enthalpies, Entropies, and Supercooling of the Prepared ILs from DSC Thermograms

phase transition <sup>a</sup>	first heating		first cooling		$\Delta S^c$ (J/mol·K)	$\Delta T_s^d$ (°C)
	$T^b$ (°C)	$\Delta H$ (kJ/mol)	$T^b$ (°C)	$\Delta H$ (kJ/mol)		
			1. C <sub>6</sub> -CPTS			
Cr <sub>1</sub> -Cr <sub>2</sub>	50.5	9.6	41.4	9.4	<i>e</i>	<i>e</i>
Cr <sub>2</sub> -Cr <sub>3</sub>	85.2	4.7	84.1	4.5	<i>e</i>	<i>e</i>
Cr <sub>3</sub> -I	95.1	21.7	92.9	20.6	59.0	2.2
			2. C <sub>8</sub> -CPTS			
Cr <sub>1</sub> -Cr <sub>2</sub>	83.5	19.0	77.5	19.8	<i>e</i>	<i>e</i>
Cr <sub>2</sub> -I	96.2	17.5	<i>e</i>	<i>e</i>	47.5	6.0
SmA-I	<i>e</i>	<i>e</i>	97.3	2.4	<i>e</i>	<i>e</i>
SmA-Cr <sub>2</sub>	<i>e</i>	<i>e</i>	93.6	15.6	<i>e</i>	<i>e</i>
			3. C <sub>10</sub> -CPTS			
Cr <sub>1</sub> -Cr <sub>2</sub>	91.8	24.6	84.5	26.3	<i>e</i>	<i>e</i>
Cr <sub>2</sub> -SmA	97.8	19.1	93.3	16.9	51.4	7.3
SmA-I	109.0	2.3	108.2	2.6	5.9	<i>e</i>
			4. C <sub>12</sub> -CPTS			
Cr-SmA	97.8	52.4	95.3	51.7	141.3	2.5
(second cycle)	(97.8)	(52.4)	(95.3)	(51.7)	(141.3)	(2.5)
SmA-I	117.9	2.2	117.4	2.3	5.7	<i>e</i>
(second cycle)	(117.9)	(2.2)	(117.4)	(2.3)	(5.7)	<i>e</i>
			5. C <sub>16</sub> -CPTS			
Cr-SmA	104.0	70.8	101.6	70.5	187.8	2.4
SmA-I	128.6	1.9	127.8	2.0	4.7	<i>e</i>
			6. C <sub>18</sub> -CPTS			
Cr-SmA	106.0	83.1	103.4	82.2	219.3	2.6
(second cycle)	(106.0)	(83.1)	(103.4)	(82.2)	(219.3)	(2.6)
SmA-I	131.6	(1.9)	131.0	2.0	4.8	<i>e</i>
(second cycle)	(131.6)	(1.9)	(131.0)	(2.0)	(4.8)	<i>e</i>
			7. C <sub>6</sub> -CPMS			
Cr-I	127.4	36.1	100.8	34.4	90.2	26.6
			8. C <sub>16</sub> -CPMS			
Cr-SmA	113.1	38.5	109.0	39.2	99.7	4.1
(second cycle)	(113.1)	38.5	(110.7)	(39.1)	(99.7)	(2.4)
SmA-I	135.2	0.7	134.4	0.7	1.8	<i>e</i>
(second cycle)	(135.2)	(0.7)	(134.4)	(0.7)	(1.8)	<i>e</i>
			9. C <sub>18</sub> -CPMS			
Cr <sub>1</sub> -Cr <sub>2</sub>	62.0	5.4	60.2	5.5	<i>e</i>	<i>e</i>
Cr <sub>2</sub> -I	111.6	37.8	<i>e</i>	<i>e</i>	98.3	2.7
SmA-I	<i>e</i>	<i>e</i>	117.6	0.4	<i>e</i>	<i>e</i>
SmA-Cr <sub>2</sub>	<i>e</i>	<i>e</i>	108.9	38.9	<i>e</i>	<i>e</i>

<sup>a</sup> Cr, Cr<sub>1</sub>, Cr<sub>2</sub>, and Cr<sub>3</sub>, crystalline phases; SmA, smectic A phase; I, isotropic phase. <sup>b</sup> Peak onset. <sup>c</sup>  $S$  was calculated from the heating enthalpy ( $\Delta H$ ) and melting point or clearing point ( $T_{cp}$ ). <sup>d</sup>  $\Delta T_s = T_{mp} - T_{fp}$  ( $T_{mp}$  = melting point,  $T_{fp}$  = freezing point). <sup>e</sup> No transition was observed.

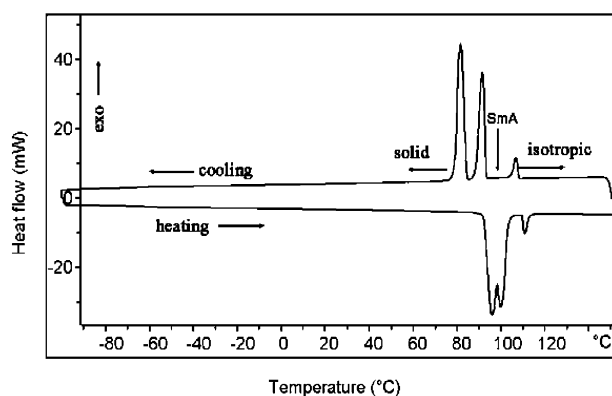


Figure 2. DSC thermogram of C<sub>10</sub>-CPTS. The sample was cooled from the isotropic liquid melted at 150 °C and then heated.

crystalline phase into liquid and then crystallized on cooling. A typical phase transition of the C<sub>18</sub>-CPTS IL is displayed in Figure 3 and can be entirely reproduced in subsequent cycles; that is, the first and second cooling–heating DSC curves are fully superposable. All the thermograms (except for C<sub>18</sub>-CPMS) contain two phase transitions with the higher 38.5–83.1 kJ/mol values and another lower enthalpy values 0.7–2.2 kJ/mol, (sections 4–6 and 8 in Table 1).

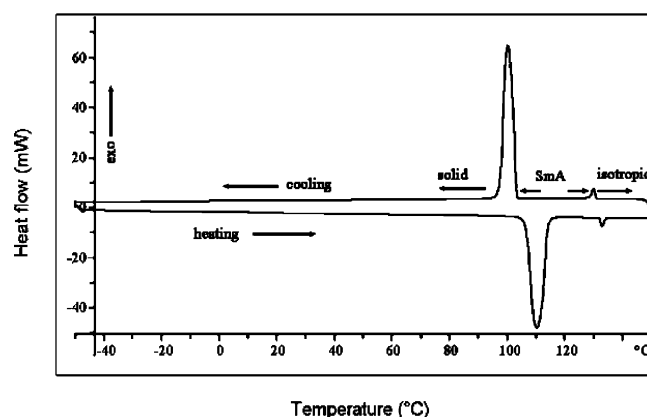


Figure 3. DSC thermogram of C<sub>18</sub>-CPTS. The sample was cooled from the isotropic liquid melted at 150 °C and then heated.

For the ILs containing [TS]<sup>-</sup>, the transition enthalpies and entropies during heating or cooling increased remarkably with increasing C number of the alkyl chain. The transition enthalpies and entropies during heating or cooling were, however, less affected by the variations of the length of alkyl chain for the ILs containing [MS]<sup>-</sup>. This means that the structure and size of anions of these ILs may play an

**Table 2. Some Properties of the  $C_n$ -CPTS and  $C_{16}$ -CPMS ILs, Therminol VP-1, [EMIm]BF<sub>4</sub>, and [BMIm]BF<sub>4</sub>**

IL	$C_p^a$ (J/g·K)	$\rho^b$ (g/mL)	$E_s^c$ sensible, $\Delta T = 100$ °C (MJ/m <sup>3</sup> )	$E_l^d$ latent (MJ/m <sup>3</sup> )
C <sub>12</sub> -CPTS	2.44	0.982	239.6	113.3
C <sub>16</sub> -CPTS	2.85	0.922	262.8	128.1
C <sub>18</sub> -CPTS	2.62	0.945	247.6	146.0
C <sub>16</sub> -CPMS	1.96	0.892	174.8	79.2
Therminol VP-1	1.78	1.060	188.7	103.1
[EMIm]BF <sub>4</sub>	1.28	1.253	160.9	60.4
[BMIm]BF <sub>4</sub>	1.66	1.175	194.9	

<sup>a</sup>  $C_p$  was measured at 145 °C for  $C_n$ -CPTS and  $C_n$ -CPMS and at 100 °C for Therminol VP-1, [EMIm]BF<sub>4</sub>, and [BMIm]BF<sub>4</sub>. <sup>b</sup>  $\rho$  was measured at 130 °C for  $C_n$ -CPTS and  $C_n$ -CPMS, at room temperature for Therminol VP-1, and at 60 °C for [EMIm]BF<sub>4</sub> and [BMIm]BF<sub>4</sub>. <sup>c</sup>  $E_s = \rho C_p \Delta T$ . <sup>d</sup>  $E_l = \rho \Delta H$

important role in the variations of the transition enthalpies. Since the transition entropies during heating or cooling increased remarkably with increasing C number of the alkyl chain over the ILs containing [TS]<sup>-</sup>, it can be conjectured that the alkyl chain became more orientated when the C number increased to  $n = 16$  or 18, and the increase of enthalpies was derived from the increased length of the alkyl chain or, more precisely, caused by the melting of the ordered alkyl chain in which more energy may be incorporated. Although that one H<sub>2</sub>O molecule contained in the ionic compound could also make some contribution to the enthalpy, such a contribution should be less than 10%. Such an oriented long alkyl chain may not be formed in the ILs containing [MS]<sup>-</sup>, although the detailed mechanism is not yet clear at this stage. It is worth noting that the most attractive properties of these caprolactam-based ILs are that high transition enthalpies are observed; for example, the C<sub>18</sub>-CPTS IL possesses 83.1 kJ/mol melting enthalpy and 82.2 kJ/mol freezing enthalpy. These, to the best of our knowledge, should be the highest transition enthalpies of ILs reported in previous literature.

The heat capacities ( $C_p$ ), densities ( $\rho$ ), and heat storage densities ( $E$ ) of some ILs are listed in Table 2, including Therminol VP-1<sup>26</sup> (a commercial heat-transfer fluid and heat storage medium<sup>27</sup>), [EMIm]BF<sub>4</sub>, and [BMIm]BF<sub>4</sub><sup>28</sup> for the purpose of comparison. It was noteworthy that all the comparative data were obtained in their liquid phases. The heat capacities were measured at 145 °C, above which the samples were liquids without any occurrence of enthalpy or glass transitions. It can be seen that variation of anions may have stronger impact on the heat capacities and that the C<sub>16</sub>-CPTS sample gives the largest heat capacities ( $C_p = 2.85$  J/g·K). Although the heat capacities of Therminol VP-1, [EMIm]BF<sub>4</sub>, and [BMIm]BF<sub>4</sub> would increase as temperature increased, such temperature dependence is relatively weak.<sup>28</sup> So, the heat capacities of  $C_n$ -CPTS ( $n = 12, 16, \text{ or } 18$ ) should be much higher than that of Therminol VP-1, [EMIm]BF<sub>4</sub>, and [BMIm]BF<sub>4</sub>. Sensible heat storage density ( $E_s$ ) is

a crucial quantity for thermal energy collection. The  $E_s$  values of the  $C_n$ -CPTS ILs are much higher than the 1.9 MJ/m<sup>3</sup> minimum specified by the American National Renewable Energy Laboratory<sup>29</sup> if a range of 100 °C was roughly chosen, and also, the latent heat storage densities ( $E_l$ ) are larger than that for the comparative materials.

**Polarizing Optical Microscopy.** The ILs were also observed by POM according to the DSC thermograms at different temperatures. The shorter-chain ILs ( $n = 6$ ), for example, C<sub>6</sub>-CPTS, melted from solid into isotropic liquid directly ca. 95 °C (melting point) upon heating. Upon cooling from isotropic liquid (Figure 4a), a texture of anisotropic crystal occurred at 80 °C. However, for the ILs with longer alkyl chains ( $n \geq 8$ ), more interesting textures were exhibited during either heating or cooling; for example, when the C<sub>18</sub>-CPTS was heated to 106 °C (melting point), a texture of anisotropic liquid, not isotropic liquid, was observed at 113 °C (Figure 4b), since changes in the brightness and/or the color are the surface features of anisotropic liquid or crystal, while isotropic phase gives a uniform and dull color. Upon further heating to 135 °C, an isotropic phase, as expected, was observed. It is worth noting that focal-conic fan textures, a common feature of smectic A phases (SmA),<sup>30</sup> appeared when the C<sub>18</sub>-CPTS IL was cooled from 135 °C (the isotropic phase) to ca. 108 °C (Figure 4c). Upon cooling to ca. 95 °C, such focal-conic fan textures disappeared entirely, and the sample became solid phase with changes in the brightness and/or the color on the surface; that is, anisotropic crystal was formed.

**X-ray Diffraction.** To obtain a better understanding of the temperature dependence of structural changes, variable-temperature powder X-ray diffraction of these ILs was further performed, and the typical XRD patterns for C<sub>18</sub>-CPTS at variable temperatures are shown in Figure 5. It can be seen that the XRD pattern (Figure 5a) consists of many sharp reflections within  $2\theta = 3\text{--}30^\circ$ , indicating that the sample structure at solid phase (95 °C) is highly ordered. Up to 125 °C (Figure 5b), the XRD pattern of the salt in its liquid-crystalline phase consists of a very broad, high-angle peak near  $2\theta \sim 19.3^\circ$  and one narrow low-angle peak at  $2\theta = 5.0^\circ$ . On the basis of XRD results, calculation with Bragg's law, and POM, C<sub>18</sub>-CPTS in its liquid-crystalline phase is the characteristic of a SmA phase with intralamellar spacing  $D = 4.6$  Å and lamellar thickness  $d = 17.6$  Å.

On the basis of DSC, POM, and XRD results, the caprolactam-based ILs with shorter alkyl chains ( $n = 6$ ) exhibited only a crystal-liquid transition without mesophase upon either heating or cooling. For  $n \geq 8$ , the ILs had completely different phase behaviors. From DSC thermograms, besides the enthalpy transitions with higher values, additional enthalpy transitions with relatively lower values could be observed at temperatures ranging ca. 109.0–135.2 °C, suggesting that isotropic liquid may not occur before or after that huge enthalpy transitions during cooling or heating. This showed some evidence that these ILs possess

(26) Therminol VP-1 Heat-transfer fluid by Solutia. Technical Bulletin 7239115B; on Therminol Reference Disk available from Solutia Inc.; <http://www.therminol.com/>.

(27) Thermal Storage for Solar Thermal Parabolic Trough Electric Power Systems. National Renewable Energy Laboratory, Request for Proposal Number RCQ-0-30910, March 27, 2000.

(28) Valkenburg, M. E. V.; Vaughn, R. L.; Williams, M.; Wilkes, J. S. *Thermochim. Acta* **2005**, *425*, 181.

(29) Holbrey, J. D.; Seddon, K. R. *Dalton Trans.* **1999**, 2133.

(30) Demus, D.; Goodby, J.; Gray, G. W.; Speiss, H.-W.; Vill, V. *Handbook of Liquid Crystals, High Molecular Weight Liquid Crystals*, Wiley-VCH: New York, 1988; p 3.

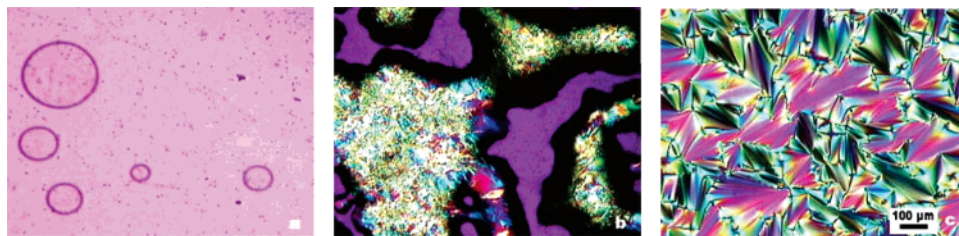


**Figure 4.** Optical micrographs of (a)  $C_6$ -CPTS and (b, c)  $C_{18}$ -CPTS at various temperatures. (a) Isotropic liquid at 110 °C upon heating (the circles are air bubbles). (b) Texture of anisotropic crystal at 113 °C upon heating. (c) Typical focal-conic fanlike texture of SmA at 108 °C upon cooling from the isotropic liquid. (The distance bar applies to the three micrographs, crossed polarizers, magnification  $\times 40$ .)

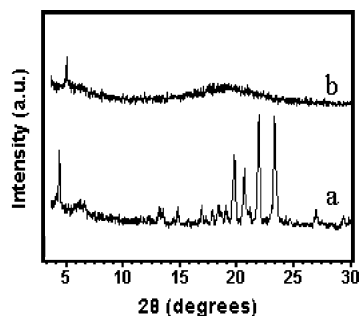


**Figure 5.** Variable-temperature PXRD patterns of  $C_{18}$ -CPTS measured at (a) 95 °C, crystal, and (b) 125 °C, SmA, upon heating.

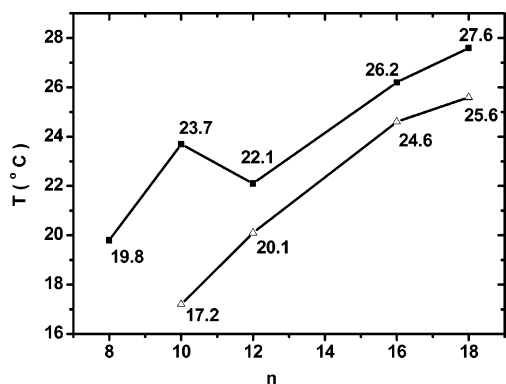


**Figure 6.** Comparison of the SmA-crystal phase transition temperature range on heating ( $\Delta$ ) and cooling ( $\blacksquare$ ) vs the number of carbon atoms ( $n$ ) in the alkyl chains of  $C_n$ -CPTS ( $n = 8-18$ ).

liquid crystal behavior. Moreover, the ILs with longer alkyl chain developed a gradually wide mesophase range  $T_{Cr-I}$ ; that is, liquid-crystalline ranges between melting and clearing points ( $T_{Cr-I} = T_{cp} - T_{mp}$ ), from 19.8 to 27.6 °C on cooling and from 17.2 to 25.6 °C on heating with increasing alkyl chain length; only the exception of  $C_{10}$ -CPTS IL slightly deviated from this general trend on cooling (Figure 6). On the other hand, the reversible occurrence of the mesophase ranges upon both heating and cooling indicated that the caprolactam-based ILCs were enantiotropic. Also, the texture of anisotropic mesophase upon heating and the typical SmA upon cooling have been observed by POM. Further XRD measurement confirmed that these ILs with longer alkyl chain either in solid or in SmA phase possessed crystal or ordered structures. So, the longer-chain ILs ( $n \geq 8$ ) exhibited enantiotropic thermotropic liquid-crystalline phases (SmA) upon heating and cooling, except for  $C_{18}$ -CPMS (monotropic).

**Fluorescence Spectra.** All the homologous  $C_n$ -CPTS ILs exhibited similar emission characteristics, which were strongly dependent on the excitation wavelengths. The typical fluo-

**Table 3. Results of the Acute Toxicity Test**

rats	$n^a/t^b$	concentrations (mg/mL)			
		100	75	50	10
$C_6$ -CPTS					
male (5)	$n$	0	0	0	0
	$t$	$c$	$c$	$c$	$c$
female (5)	$n$	0	0	0	0
	$t$	$c$	$c$	$c$	$c$
$C_{18}$ -CPTS					
male (5)	$n$		0	0	0
	$t$		$c$	$c$	$c$
female (5)	$n$		0	0	0
	$t$		$c$	$c$	$c$
$C_6$ -CPMS					
male (5)	$n$	0	0	0	0
	$t$	$c$	$c$	$c$	$c$
female (5)	$n$	0	0	0	0
	$t$	$c$	$c$	$c$	$c$
$C_{18}$ -CPMS					
male (5)	$n$		0	0	0
	$t$		$c$	$c$	$c$
female (5)	$n$		0	0	0
	$t$		$c$	$c$	$c$
[BMIm]BF <sub>4</sub>					
male (5)	$n$			5	3
	$t$		2 h	5 h	48 h
female (5)	$n$			5	4
	$t$		1 h	2 h	48 h

<sup>a</sup>  $n$  indicates the death number of the rats. <sup>b</sup>  $t$  indicates the living time of the rats. <sup>c</sup> No death occurs within 7 days.

rescence behavior of neat  $C_6$ -CPTS and  $C_{16}$ -CPTS is displayed in Figure 7. No fluorescence could be observed when excitation wavelengths were below 224 nm or above 280 nm. The fluorescence appeared and became fairly strong, with an emission band centered around 289 nm, and then the intensity decreased quickly with the maximum emission band keeping constant as excitation wavelengths increased from 224 to 280 nm. Also, it is worth noting that much higher quantum yields could be achieved when the excitation wavelengths were around 264 nm. It can be seen that the intensity of the emission was affected by the alkyl chain length on the caprolactam cation, but the emission peak position hardly changed at  $\lambda_{em} = 289$  nm. When [TS]<sup>-</sup> was substituted with [MS]<sup>-</sup> anion, no fluorescence behavior was observed; that is, anion as illuminophore made a greater contribution to the fluorescence behavior.

**Toxicity.** It is essential to understand the toxicity of the new materials and their impact on the environment when they go to industrial and commercial applications. In order to know the toxicity of the caprolactam-based ILs, a preliminary experiment comparing the toxicity of the four ILs containing [TS]<sup>-</sup> or [MS]<sup>-</sup> anion with shorter or longer chains, and [BMIm]BF<sub>4</sub> for the purpose of comparison, have been conducted by measuring acute toxicity

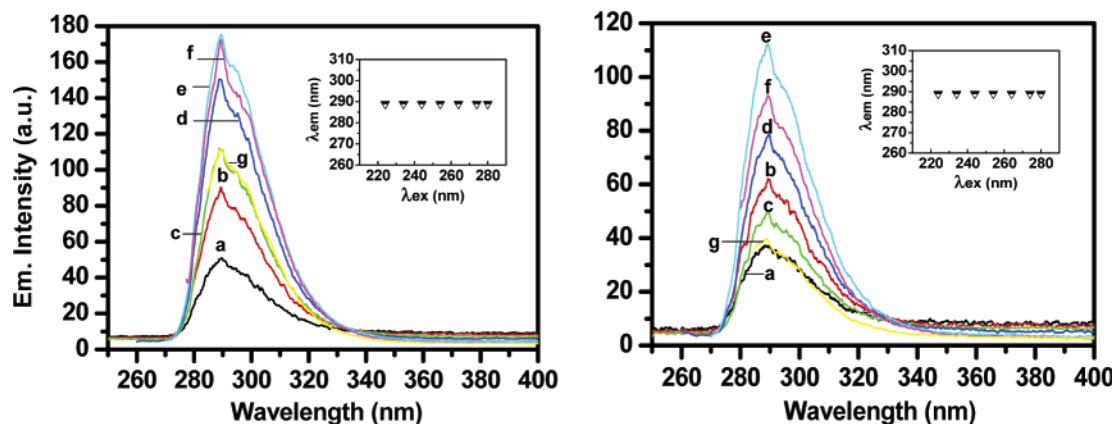


**Figure 7.** Excitation wavelength-dependent emission behavior of neat C<sub>6</sub>-CPTS (left) and C<sub>16</sub>-CPTS (right).  $\lambda_{\text{ex}}$  (in nanometers) = 224 (a), 234 (b), 244 (c), 254 (d), 264 (e), 274 (f), and 280 (g). The insets show the emission wavelengths at the fluorescence maxima vs the corresponding excitation wavelengths of neat C<sub>6</sub>-CPTS (left) and C<sub>16</sub>-CPTS (right).

toward Kunming albino rats (Figure S8, Supporting Information).

As shown in Table 3, no rat death was observed when the concentrations of the solutions containing C<sub>6</sub>-CPMS/C<sub>6</sub>-CPTS and C<sub>18</sub>-CPTS/C<sub>18</sub>-CPMS were lower than 100 mg/mL and 75 mg/mL, respectively. For the purpose of comparison, the same test of acute toxicity for the conventional [BMIm]BF<sub>4</sub> IL, which was thought to be not acutely toxic,<sup>31</sup> was also conducted. However, all the rats died in 10 min to 5 h after 0.4 mL of the solution containing  $\geq 50$  mg/mL of [BMIm]BF<sub>4</sub> was fed. The result showed that the toxicity of the caprolactam-based ILs was lower than that of [BMIm]BF<sub>4</sub>. Therefore, they could be thought to be a kind of environment-friendly ILs.

### Conclusions

A series of novel ILs based on *N*-alkyl- $\epsilon$ -caprolactam as cations were synthesized with a one-step atom-economic

reaction for the first time. The ILs ( $n \geq 8$ ) exhibited enantiotropic thermotropic liquid-crystalline phases SmA, except for C<sub>18</sub>-CPMS (monotropic). Some interesting and favorable properties, such as the highest transition enthalpies among the reported ILs, higher specific heat capacities, and higher heat storage densities, were observed. Also, the caprolactam-based ILs have proven to be less toxic than the popular [BMIm]BF<sub>4</sub> IL. On the basis of their properties, safety, and relatively lower cost, the novel liquid crystalline materials may have potential applications as optoelectronic materials, thermal storage media, or ordered reaction media.

**Acknowledgment.** We gratefully acknowledge financial support from the National Natural Science Foundation of China (20533080, 20225309, and 60377039).

**Supporting Information Available:** Experimental details with <sup>1</sup>H NMR, ESI-MS, FT-IR and elemental analyses and toxicity test (PDF). This material is available free of charge via the Internet at <http://pubs.acs.org>.

CM062675S

(31) (a) Swatloski, R. P.; Holbrey, J. D.; Memon, S. B.; Caldwell, G. A.; Caldwell, K. A.; Rogers, R. D. *Chem. Commun.* **2004**, 668. (b) Pernak, J.; Czepukowicz, A. *Ind. Eng. Chem. Res.* **2001**, *40*, 2379.